ION EXTRACTION FROM GAS CELLS WITH SUPERSONIC JETS FORMED IN LAVAL NOZZLES

Alexandru STATE[1,2], Mihai MERISANU[3], Dimiter L. BALABANSKI[2,3], Paul CONSTANTIN[3], Tiberiu SAVA[1], Adrian ROTARU[1], Traian ROMAN[3], Dragoș NICHITA[2,3], Anamaria SPĂTARU[2,3], Wolfgang R. PLAß[4,5]

The proposed IGISOL setup at Extreme Light Infrastructure – Nuclear Physics (ELI-NP) will generate radioactive ions via photo-fission of uranium targets placed inside a two-chamber gas cell. In the final stages of their extraction from the cell, i.e. between the first and the second chamber of the cell and the exit of the second chamber, the ions are dragged and carried by supersonic gas jets formed at the exit of Laval type nozzles. Computational fluid dynamics (CFD) gas flow simulations have been performed to establish the gas velocity, temperature and pressure distributions that describe the overall behavior of these supersonic jets.

Keywords: IGISOL, Cryogenic Stopping Cell, Laval nozzle, supersonic jet.

1. Introduction

The recent developments regarding the ELI-NP (Extreme Light Infrastructure-Nuclear Physics) project [1] bring it closer to the operational stage where two important equipment will be of utmost importance: the high-power laser system with two 10PW ultra-short pulse lasers and a highly brilliant gamma-ray beam system, with energies up to 19.5MeV [2]. The latter will provide a new research instrument of worldwide importance in which the gamma beam energies will cover the GDR (Giant Dipole Resonance) of Uranium and Thorium isotopes making it ideal for photo-fission experiments [3][4].

The IGISOL setup (Ion Guide Isotope Separator On-Line) [5] is one of the proposed experimental setups that will make use of the gamma beam system. An important component of the IGISOL is the High Areal Density Orthogonal

[1] Horia Hulubei National Institute for Physics and Nuclear Engineering, 30 Reactorului Street, 077125 Bucharest, Măgurele, Romania, e-mail: alexandru.state@nipne.ro
[2] Doctoral School in Engineering and Applications of Lasers and Accelerators, University POLITECHNICA of Bucharest, Romania.
[3] Extreme Light Infrastructure – Nuclear Physics, ''Horia Hulubei" National Institute for Physics and Nuclear Engineering, Str. Reactorului 30, 077125 Bucharest Măgurele, Romania
[4] II. Physikalisches Institut, Justus-Liebig-Universitat Gießen, 35392 Gießen, Germany
[5] GSI Helmholtzzentrum fur Schwerionenforschung GmbH, 64291 Darmstadt, Germany

Extraction Cryogenic Stopping Cell (HADO-CSC), a two-chamber gas cell with orthogonal extraction, which provides short extraction times in the range of milliseconds. [6]. Such a design has been firstly proposed to be used with the Super-FRS at GSI [7], being an upgrade of the existing one [8].

The conceptual design of the CSC is emphasized in Fig. 1. In the helium gas, the fission products undergo a thermalization process in which a large fraction of the reaction products reach a 1^+ charge state [9]. Strong DC fields ($\approx 100 V/cm$) drift the ions out in an orthogonal direction to the impinging gamma beam. Close to the cell wall, resonant RF fields will prevent their adhesion to the wall and push them towards the exit nozzles, where the gas flow will guide them in supersonic jets. The operational conditions of the cell imply a cryogenic temperature (70-80 K), for an increased gas density and purity, and high pressure (200-300 mbar) in the lower stopping chamber and low pressure (3-10 mbar) in the upper extraction chamber.

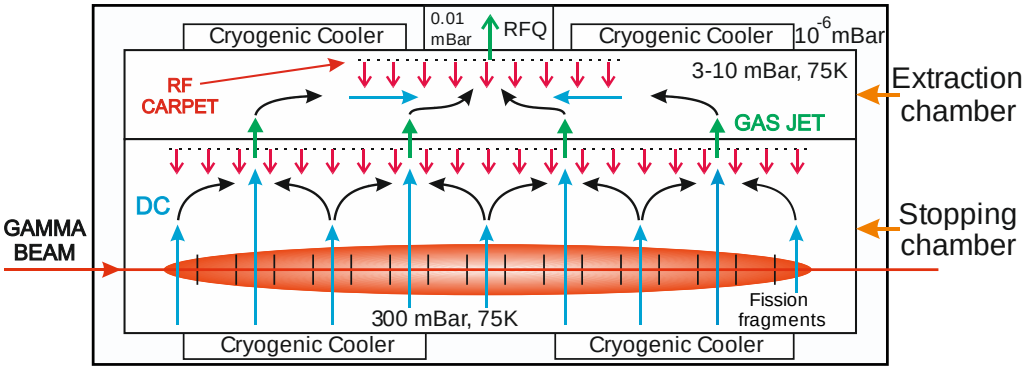

Fig. 1. Conceptual design of the CSC: photo-fission region in red, ion trajectories in black, DC fields in blue, RF fields in red, gas jets in green [7].

This paper presents first estimations for the gas jet parameters inside of small Laval nozzles, designed considering the quasi-one-dimensional flow equations. The transport of heavy ions produced via photo-fission by the supersonic gas jets has been investigated, as well.

2. Supersonic isentropic flow equations

The flow of a compressible, inviscid fluid is described by three dynamic equations: the continuity equation, based on local mass conservation; the momentum equation, based on Newton's principle $F = m \cdot a$ and the energy equation, based on local energy conservation. In the case of isentropic flows of calorically perfect gases, which is considered here, these equations can be solved analytically.

If the flow through a nozzle is gradually compressed (area decreases) and then gradually expanded (area increases), the flow conditions return to their original

values. Such a process is reversible. The second law of thermodynamics implies that a reversible flow maintains a constant value of entropy. Such a flow is defined as an isentropic flow. Isentropic flows occur when the changes in flow variables are small and gradual, such as an ideal flow through a nozzle.

A flow is considered supersonic when the Mach number (ratio of flow velocity over the speed of sound in that medium) is higher than one. Converging-diverging nozzles, sometimes called de Laval (or Laval) nozzles [10], have been considered as the transport route for the created ions in the photo-fission mechanism, considering that such nozzles are mainly used to accelerate gases into supersonic jets. The schematic design of the considered nozzle is presented in Figure 2 and has the dimensions given in Table 1. The diverging section is described by an arc given by the circle of radius r and the converging section is described by two straight lines at A and B angles. The lengths of the different sections are denoted by L_i, $i = 1,2,3$ and the diameters of the inlet, outlet and the nozzle throat are denoted by d_1, d_2 and d_t, respectively. In Figure 2, T_{in} is the inlet temperature and P_{in}, P_{out} are the inlet and outlet pressures. The inlet values correspond to the stopping section whilst the outlet values correspond to the extraction section.

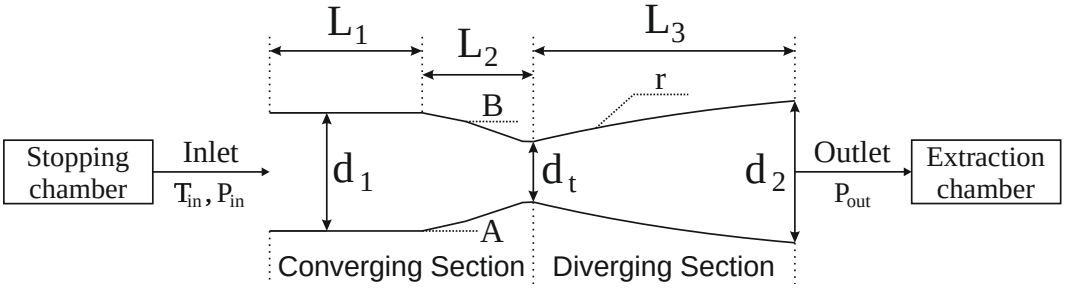

Fig. 2. Schematic design of the Laval nozzle.

Table 1

Parameters of the Laval nozzle geometry (see definitions in the text)

L_1[mm]	L_2[mm]	L_3[mm]	d_1[mm]	d_2[mm]	d_t[mm]	A[°]	B[°]	r[mm]
0.754	0.596	1.35	0.6	0.72	0.3	11.754	20.487	8.3

The resulting properties of the gas jets depend on the nozzle shape and the pressure boundaries. Gas jets expansion phenomena and nozzle design are treated in detail in Ref. [10]. The main characteristics of the transition from a subsonic to a supersonic flow regime in a Laval nozzle, can be described in a quasi-one-dimensional symmetry. Considering the assumptions for the flow described above, the change in velocity can be expressed in terms of the Mach number M by the area-velocity relation:

$$\frac{dA}{A} = (M^2 - 1)\frac{dv}{v} \tag{1}$$

where v represents the velocity of the gas and A the area of the enclosing structure.

From Equation 1 it results that the gas velocity is solely determined by the nozzle geometry. Consequently, the speed of sound, at $M = 1$, can only be reached at the nozzle throat where $dA = 0$. In a Laval nozzle as the subsonic flow enters the nozzle and the area decreases: $dA < 0$, the flow accelerates because $M < 1$ until the smallest radius, i.e. the throat, is reached and M becomes 1. After the throat, dA becomes positive, as well as $M > 1$, such that the acceleration continues into a supersonic flow.

Equation 1, under the assumption of a calorically perfect gas, can be explicitly solved to obtain the area-Mach number equation:

$$\left(\frac{A}{A_t}\right)^2 = \frac{1}{M^2}\left[\frac{2}{\gamma+1}\left(1+\frac{\gamma-1}{2}M^2\right)\right]^{\frac{\gamma+1}{\gamma-1}} \tag{2}$$

where A_t is the nozzle throat area which has to be smaller than A and γ represents the ratio of specific heats, i.e. c_p over c_v. The suffixes in the latter two terms P and V refer to constant pressure and constant volume conditions. For every value of A ($A \geq A_t$) two real solutions fulfil Equation 2, corresponding to a subsonic and a supersonic value, as seen in Fig. 3.

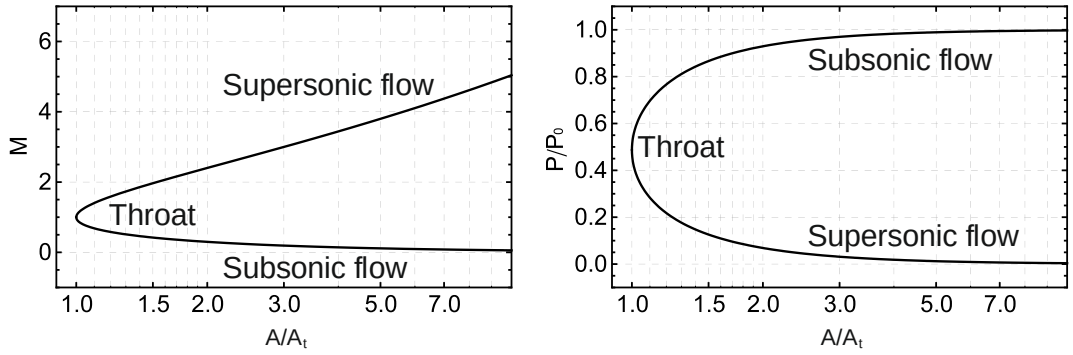

Fig. 3. Gas jet velocity evolution from subsonic to supersonic as a function of the area ratio (left); Pressure ratio as a function of area ratio in the transition from subsonic to supersonic (right).

Using the Mach number distribution, the temperature, pressure and density distributions can be established. The jet pressure and temperature equations are:

$$\frac{P}{P_0} = \left(1+\frac{\gamma-1}{2}M^2\right)^{\frac{-\gamma}{\gamma-1}} \tag{3}$$

$$\frac{T}{T_0} = \left(1 + \frac{\gamma - 1}{2} M^2\right)^{-1} \tag{4}$$

where P_0 and T_0 represent the total pressure and total temperature for $M = 0$, which correspond in our case to the pressure and temperature inside the stopping chamber of the gas cell. For a monoatomic gas, like helium, $\gamma = 5/3$ and the parameter ratios at the throat, when $M = 1$, become $T/T_0 = 0.75$ and $P/P_0 = 0.487$.

Starting from the nozzle represented in Figure 2, an area-ratio distribution can be calculated, which in turn can be utilized in Equation 2 to obtain the Mach number distribution as a function of the distance x along the nozzle axis.

After the Mach number distribution is known, the ratio of static to total pressure or temperature can be obtained using Equations 3 and 4. These correlations are plotted in Figure 4 and represent the first theoretical approximation of the flow parameters inside the nozzle. This step is called the design stage.

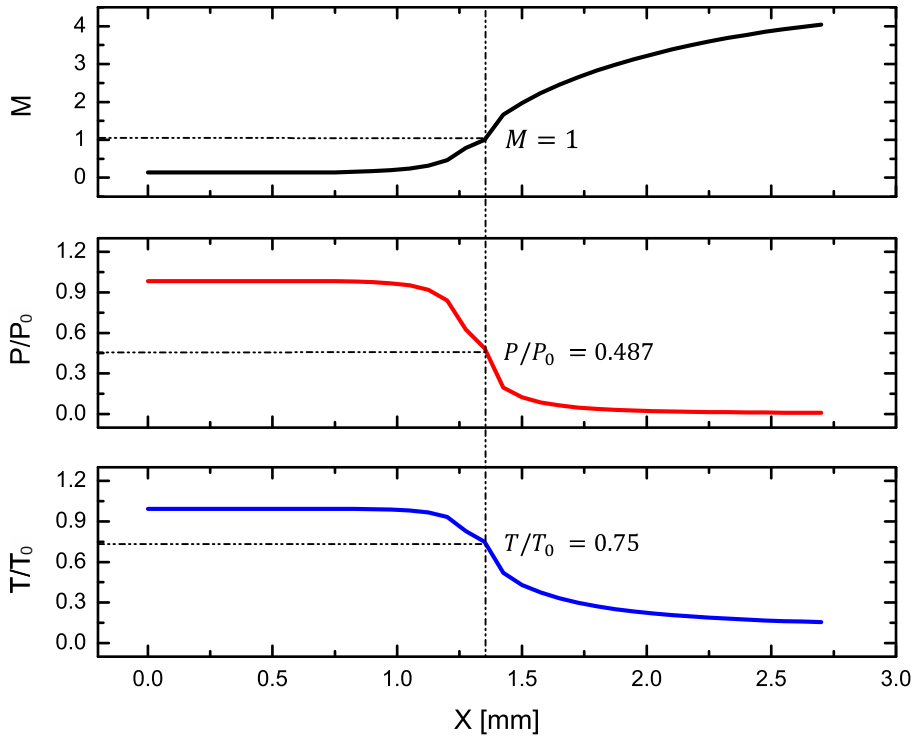

Fig. 4. The dependence on the distance x along the nozzle axis of the Mach number (top), total to static pressure (middle), and total to static temperature (bottom).

At $x = 1.35$ mm, i.e. at the throat location, the flow turns supersonic as the gas jet velocity is continually increasing. Therefore, from this point forward we consider the supersonic solution from the two solutions that result from Equation 2. By knowing the idealized theoretical curves that describe the overall behaviour of

the gas flow through the jet, the input simulation parameters can be set and tested under the assumption of an idealized gas following an isentropic flow.

3. COMSOL simulations of the CSC with Laval nozzles

The CSC of the IGISOL setup at ELI-NP uses helium gas at 70-80 K and 200-300 mbar, which can be considered in a very good approximation, a calorically perfect gas. Although, there exist significant heat sources, represented by the RF electric fields of the CSC, they can be neglected in the regions inside and around the nozzles, where the CFD simulations are performed. Hence, the flow inside the gas jets is adiabatic. The last condition for isentropic flows, namely reversibility, is not met because the pressure ratio is not what is required by Equation 3. More specifically, in these simulations the gas goes from 300 mbar in the stopping chamber to 3 mbar in the extraction chamber. This leads to the formation of shocks, which will be discussed in more detail further. The flow, however, is isentropic in the nozzle region up to the shock location.

The fluid dynamics simulations have been performed using COMSOL Multiphysics©, specifically the High Mach Number Flow module [11].

Using the area ratio $A_{in}/A_t = 4$, where A_{in} is the cross-sectional area at the nozzle inlet, Equation 2 gives at the entrance in the converging section a subsonic solution $M_{in} = 0.14$ and a supersonic solution $M_{in} = 3.44$. Retaining only the physical subsonic solution for the exit from the large stopping chamber, and using its static temperature at $T_0 = 75$ K, the initial velocity of the gas jet in the nozzle is given by:

$$v_{in} = M_{in} \cdot \sqrt{\gamma R_s T} \tag{5}$$

where R_s is the specific gas constant.

The material used in the simulations is Helium and the considered properties include: a specific gas constant $R_S = 2080\ J/Kg/K$, a heat capacity at constant pressure $C_P = 5194\ J/(Kg \cdot K)$, a ratio of specific heats $\gamma = 1.667$ and a mean molar mass $M_n = 0.004\ Kg/mol$.

First, the Laval nozzle has been simulated by defining the inlet and outlet pressure boundaries of 300 mbar for the inlet and 3 mbar for the outlet, thus reproducing the pressures in the two chambers of the CSC. The simulation results, which are shown in the top panel of Fig. 5, were determined by considering the

values along the nozzle centreline. The bottom panel of this figure shows the ratio of the simulated values with the calculated ones, which were presented in Fig. 4.

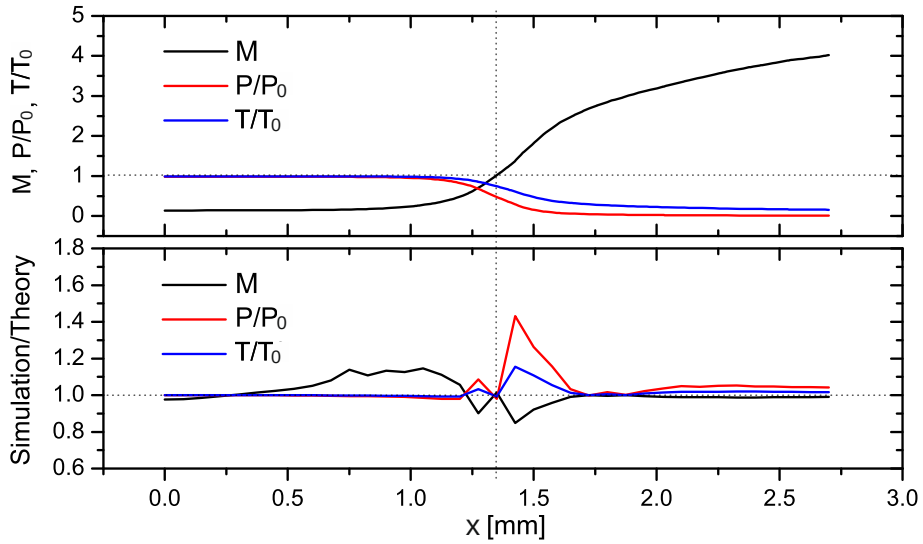

Fig. 5. (Top) Dependence of the Mach number, total to static ratios of pressure and temperature on distance x along the nozzle axis. (Bottom) Ratio of simulation results and the values obtained with the isentropic theory in the case of a calorically perfect gas.

Mach number deviations are generally larger because of the proportionality between the Mach number, velocity and temperature. From equation 5: $M \sim v/\sqrt{T}$, hence, the velocity and temperature deviations cumulate in M. At the throat, where $M = 1$, the three values of Figure 4 show less than 2% differences when compared to the theoretical values. Noticeable deviations, as seen in Figure 5 (Bottom), are immediately after the throat where the resulted value for M from the simulation has a smaller value than the theoretical one, leading to a decrease of the simulation over theory ratio for M and an increase of the pressure and temperature ratios. There are two reasons that led to these discrepancies. Firstly, the simulations take into account the small turbulences that appear at the throat edges, while the equations presented in Section 2 do not. Secondly, the 3D simulation exhibits a more real situation, where the flow line presents a curvature towards the divergent section, hence the solutions in this region will be slightly different when compared to the analytical values that assume the sonic line to be a straight line across the throat. At the nozzle outlet, a Mach number of $M_{out} = 4.03$ is obtained, which is within 0.25% of the analytic value. This high value is a combination of the acceleration to the nozzle exit velocity of $v_{out} = 805$ m/s with a temperature drop to $T_{out} = 11.5$ K.

The density and velocity distributions are presented in Fig. 6. For a supersonic, compressible flow, both the density and velocity change with area to conserve mass, hence the density starts to decrease from a value of 0.191 kg/m^3 at

the location where the convergent part starts, reaching at the exit a value of 0.0113 kg/m^3. This was to be expected considering both mass and momentum conservation: in the diverging section, as the area increases, the velocity will increase forcing the density to decrease. Of course, the mass debit of 0.226 g/min is conserved during the entire flow.

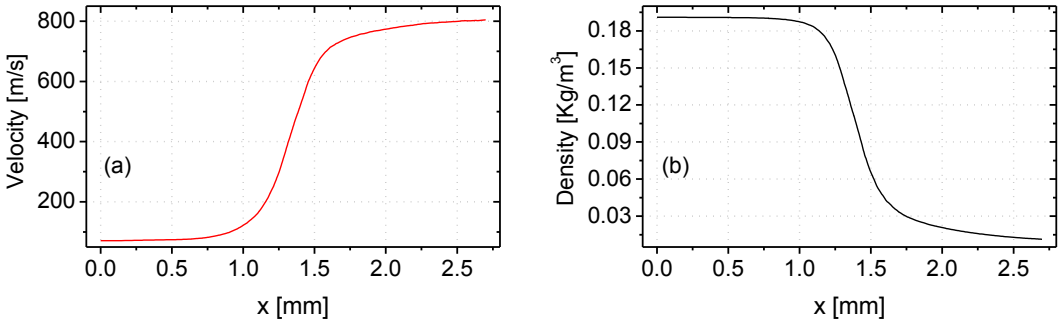

Fig. 6. Velocity (a) and density (b) distributions along the Laval nozzle.

One important aspect that should be considered is the effect the pressure ratio has over the flow. For $M_{out} = 4.03$ and $P_0 = 300$ mbar, an outlet pressure of $P_{out} = 3$ mbar is required for an isentropic flow (see Equation 3). A smaller pressure value will not lead to any difference, as the flow is chocked at the nozzle throat, hence the mass flow rate is independent of the downstream pressure. A bigger value of the pressure ratio will lead to the formation of a shock in the divergent region. Figure 7 displays the results for the 3mbar case discussed above and a case in which the outlet pressure has been modified drastically (200 mbar).

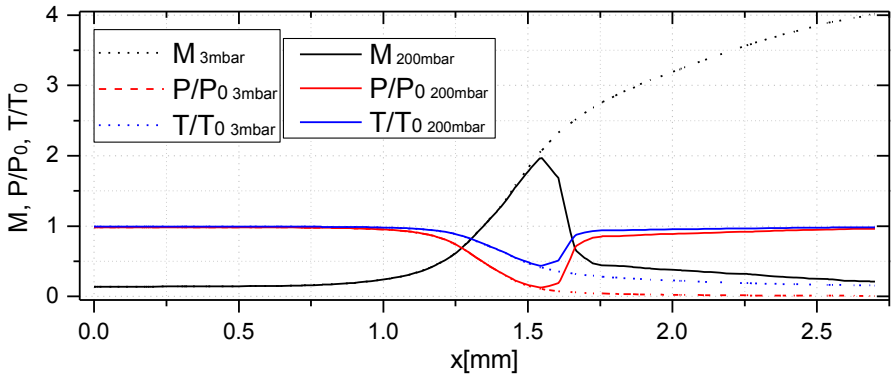

Fig. 7. Dependence of the Mach number and the total to static ratios for pressure and temperature on the distance x along the nozzle axis; 200 mbar at outlet (solid lines) and 3 mbar at outlet (dotted lines).

For a shock free isentropic supersonic flow, the ratio of exit to total pressure is defined by Equation 3 (see also Fig. 3). Since the backpressure downstream the

nozzle is created independently, pressure differences lead to the formation of shocks, either at the exit of the nozzle or a normal shock somewhere in the divergent section. This behaviour leads to a quick decrease in the Mach number and a big increase of P/P_0 and T/T_0 ratios.

Moreover, if the back pressure is too high, normal shocks are formed in the divergent part of the nozzle. Such shocks are a potential problem because they generate vibrations in the CSC wall and the generated flow discontinuities can affect the heavy ion transport. Waves, emanating from a non-perfectly expanded nozzle will reflect at the jet shear layer and the jet centreline resulting in a shock diamond pattern downstream of the nozzle exit. Such a flow is not governed anymore by the quasi one-dimensional flow equations.

So far, the Laval simulations have proven that the fluid model is within acceptable parameters when compared to the theoretical isentropic solutions. Moreover, as stated before and exemplified in Fig. 7, the outlet pressure conditions are of utmost importance. Thus, a pressure ratio different than the isentropic condition leads to the formation of shockwaves. Realistically, the inlet and outlet pressures for the Laval nozzle will take the precise values described theoretically by Equations 3 and 4, but with a consequence of the inlet and outlet conditions of the CSC gas system.

The velocity and temperature distributions within a supersonic gas jet formed with a Laval nozzle, when it is used as an ion guide inside the CSC, is presented in Fig. 8 where the nozzle is placed between the stopping chamber and the extraction chamber. The height of the extraction chamber is 10 cm.

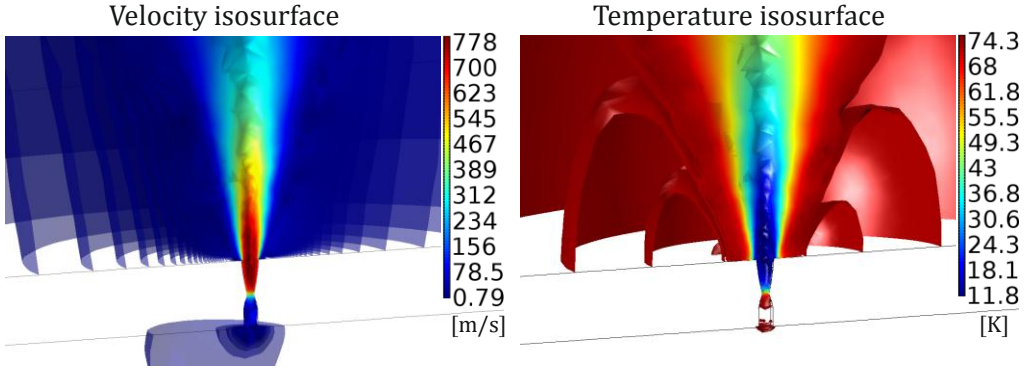

Fig. 8. Velocity isosurface (left) and temperature isosurface (right) of the formed supersonic jet in the cryogenic stopping cell with Laval nozzles.

The simulation program considers the compression and expansion effects that occur. Since the jet is slightly under expanded (nozzle outlet pressure larger than the ambient pressure, i.e. 3mbar), expansion waves are still possible leading to a second Mach peak as demonstrated in Fig. 9. This under-expansion leads to a decrease in the exit Mach number by 5% when compared to the isentropic solution.

The exit flow velocity is 792 m/s corresponding to M=3.81 at a temperature of 12.45 K and a pressure of 3.01 mbar.

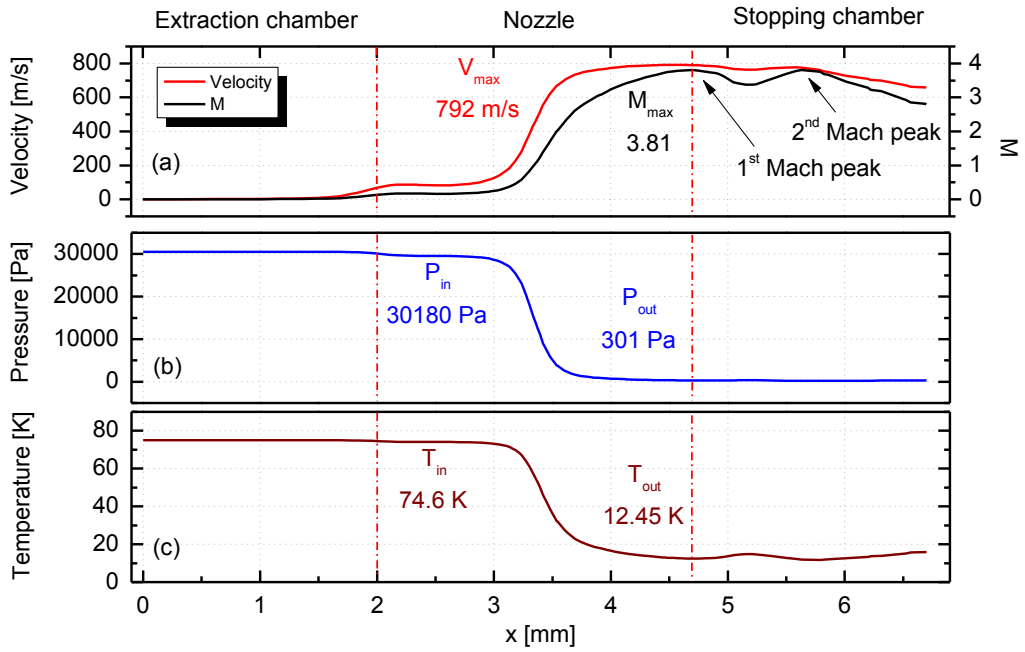

Fig. 9. (a) Velocity, Mach number, (b) temperature and (c) pressure distributions 2 mm before and after the nozzle.

4. Heavy ion transport by supersonic gas jets

The flow in the Laval nozzle presented above, can be approximated as an isentropic, adiabatic flow and the velocity field obtained can be used to simulate the transport of heavy ions generated via photo-fission by supersonic jets. One thousand ions have been released from the nozzle inlet with a uniform spatial distribution and an initial velocity equal to zero. The wall condition has been defined to freeze out the particles that get in contact with it. Ions are defined by their mass and diameter. The mass distribution covers the main regions of interest: the refractory elements in the Zr-Mo-Rh region with A≈100 and in the heavy rare earth region around Ce with A ≈ 140 [4, 6]. The particle radii for the considered isotopes, determined from minimal-basis-set SCF (Self-Consistent Field) functions, can be found in Ref. [12].

A time-dependent study has been performed covering 2 ms from the nozzle inlet to the RF carpet, with a time step of 0.5 μs. Representative isotopes for the above two regions have been considered, namely ^{89}Rb and ^{145}Ce. Fig. 10 shows the particles behaviour in the nozzle. In 20 μs all isotopes reach the nozzle outlet and tend to reach the maximum velocity obtained for the gas flow of 792 m/s.

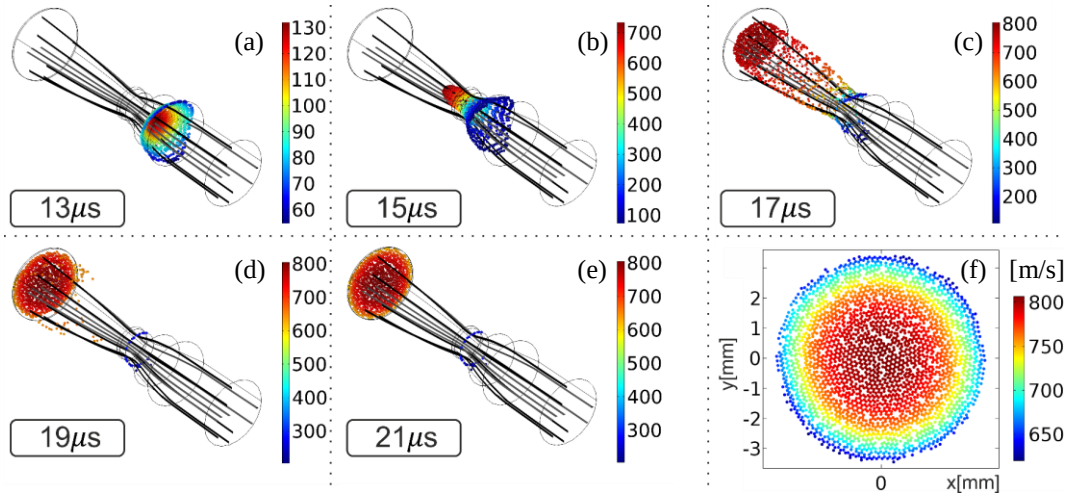

Fig. 10. Transport velocity in m/s for a thousand heavy ions at five time-steps (a, b, c, d, e) and the phase portrait (f) of the heavy ions at the nozzle outlet, colour coded by their velocity.

The ions follow the gas flow streamlines which converge towards the throat. The maximum velocity is met at the nozzle centre and it decreases towards the boundary surface. This can be seen in the phase portrait of Fig. 10. Moreover, this difference in velocity is due to the uneven pressure across the inlet surface, presenting larger values than 300 mbar near the boundary layers.

The average particle velocity in function of time for both ^{89}Rb and ^{145}Ce has been plotted in Figure 11 for the entire region from the entrance of the nozzle to the end of the extraction chamber. In this region of about 10 cm, heavy ions are transported by the gas jets rather than by electric fields. The ions reach the RF carpet on the upper wall of the extraction chamber in 1.9 ms at an average velocity of 10.2m/s. Furthermore, the transport times can be effectively decreased by an order of magnitude with the electrical fields applied.

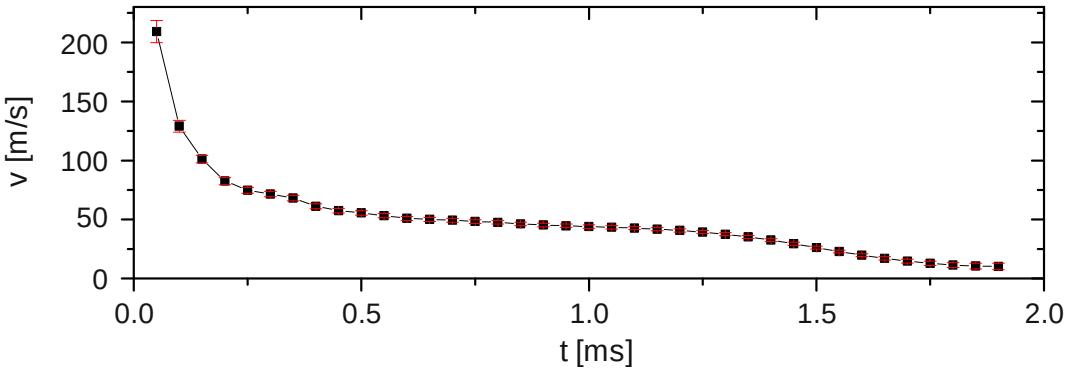

Fig. 11. Average particle velocity for ^{145}Ce and ^{89}Rb in the CSC in function of time.

5. Conclusions

This paper presents the results obtained in the investigation of the gas flow through Laval nozzles, which will be used as ion-guides for the fission fragments produced inside the CSC. The simulations are in good agreement with the theory of isentropic flow, except immediately after the nozzle throat where the flow is turbulent. The simulation results for the isentropic flow from 300 mbar to 3 mbar indicate an acceleration of the gas jets from Mach 0.1 to Mach 4, corresponding to a maximum velocity of about 800 m/s and a minimum temperature of 11.5 K.

The flow drag of the photo-fission fragments has also been investigated. These heavy ions exit the nozzles with a velocity close to that of the gas jets and are transported through the extraction chamber in about 2 ms, reaching the RF carpet with an average velocity of about 10 m/s. Further investigations are necessary to optimize the flow parameters and to include the ion drift induced by the DC fields.

The ELI-NP group was supported by the Extreme Light Infrastructure Nuclear Physics (ELI-NP) Phase II, a project co-financed by the Romanian Government and the European Union through the European Regional Development Fund the Competitiveness Operational Program (1/07.07.2016, COP, ID 1334).

The IFIN-HH group was supported by the ELI-RO project financed by the Romanian Government through the Grant Program ELI-RO-07.

R E F E R E N C E S

[1]. *N.V. Zamfir*, Nuclear Physics News, **25**, 34 (2015)
[2]. *S Gales et al*, Rep. Prog. Phys. **81**, 094301 (2018)
[3]. *D.L. Balabanski et al*, Eur. Phys. Lett. **117**, 28001 (2017)
[4]. *P. Constantin et al*, Nucl. Inst. Meth. B, **372**, 78-85 (2016)
[5]. *D.L. Balabanski et al*, Rom. Rep. Phys. **68**, S621 (2016)
[6]. *P. Constantin et al*, Nucl. Inst. Meth. B, **397**, 1-10 (2017)
[7]. *T. Dickel et al*, Nucl. Inst. Meth. B, **376**, 216-220 (2016)
[8]. *S. Purushothaman*, Eur. Phys. Lett. **104,** 42001 (2013)
[9]. *J. Äystö et al*, Nucl. Phys. A **693** 477–494, (2001)
[10]. *J.D. Anderson*, "Modern Compressible Flow With Historical Perspective", McGraw-Hill Professional, New York (2002)
[11]. COMSOL Multiphysics Reference Manual, version 5.1
[12]. *E. Clementi*, J Chem. Phys. **47**, 1300 (1967)